



# Morphological Characteristics of Molybdenum Disulfide and Current Application on Detecting SF<sub>6</sub> Decomposing Products

Guochao Qian\*, Qingjun Peng, Haozhou Wang, Shan Wang and Weiju Dai

Electric Power Science Research Institute of Yunnan Power Grid Co., Ltd., Kunming, China

## OPEN ACCESS

### Edited by:

Wen Zeng,  
Chongqing University, China

### Reviewed by:

Yanqiong Li,  
Chongqing University of Arts and  
Sciences, China

Jianbo Yin,  
Northwestern Polytechnical  
University, China

### \*Correspondence:

Guochao Qian  
164688847@qq.com

### Specialty section:

This article was submitted to  
Smart Materials,  
a section of the journal  
Frontiers in Materials

Received: 05 July 2020

Accepted: 02 September 2020

Published: 06 November 2020

### Citation:

Qian G, Peng Q, Wang H, Wang S and  
Dai W (2020) Morphological  
Characteristics of Molybdenum  
Disulfide and Current Application on  
Detecting SF<sub>6</sub>  
Decomposing Products.  
Front. Mater. 7:580245.  
doi: 10.3389/fmats.2020.580245

MoS<sub>2</sub> has been considered a potential novel material in various fields due to its large specific surface area, high carrier mobility, and tunable electronic properties. However, with the increasing demand for sensor substrates, different strategies have been made to achieve its high performance, usually by adopting the method of controlling the microstructure. SF<sub>6</sub> gas-insulated electrical equipment has gained considerable attention in electric systems with the advantages of small volume, high security, strong breaking performance, and high-pressure fracture tolerance. Nevertheless, in the process of equipment operation, the SF<sub>6</sub> gas will occur inevitably decompose due to partial discharge, resulting in the deterioration of the insulation performance of the equipment. Therefore, detecting SF<sub>6</sub> decomposition products is significant for the safe and stable operation of power systems. In this mini review, we start from the synthesis of various MoS<sub>2</sub> morphological structures. Then, the beneficial characteristics of the unique synthesized nanostructures at present are analyzed. Besides, we focus on the gas-sensing mechanisms and applications of MoS<sub>2</sub>-based sensors for detecting SF<sub>6</sub> decomposition products. Finally, the future development in this field is proposed.

**Keywords:** molybdenum disulfide, morphological characteristics, SF<sub>6</sub> decomposing products, sensing application, gas insulated switchgear

## INTRODUCTION

Sulfur hexafluoride (SF<sub>6</sub>) is a non-color, tasteless, and non-flammable insulating gas, which is widely known for applications in gas insulated switchgear (GIS) (Lu et al., 2018; Lu et al., 2019). Although GIS has advantage of high stability, insulation faults such as partial discharge, breakdown discharge, and spark discharge inevitably occur during a long running process (Zeng et al., 2015; Liu et al., 2017), which will lead to the decomposition of the SF<sub>6</sub> gas into various sulfur fluorides, including H<sub>2</sub>S, SO<sub>2</sub>, SO<sub>2</sub>F<sub>2</sub>, and SOF<sub>2</sub> etc. (Wei et al., 2020). Previous research has indicated that these characteristic gases can accelerate the corrosion rate of facilities and increase the probability of system paralysis (Zhang X. X. et al., 2017a; Zhou et al., 2018b). Therefore, it is of great necessity to evaluate the operational status of GIS equipment by effectively detecting these typically decomposed products of SF<sub>6</sub> (Zhang X. X. et al., 2017b; Zhou et al., 2018d). In this respect, bidimensional nanomaterials have captured widespread attention for its multiple physical and chemical properties in the detection of SF<sub>6</sub> decomposed gas (Zhou et al., 2018a; Chen et al., 2018).

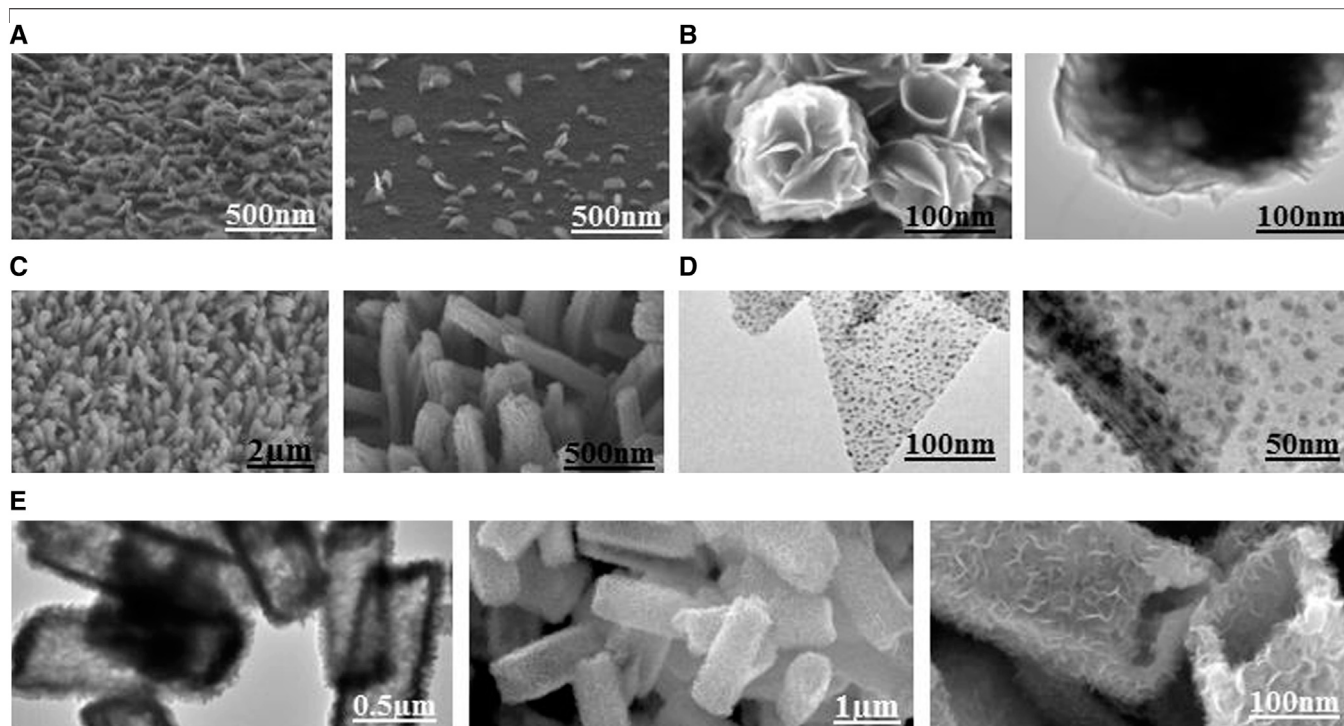


**FIGURE 1** | MoS<sub>2</sub> with different hierarchical structures: **(A)** Vertical nanoflakes. Reprinted with permission from Kang et al. (2017). Copyright (2017) American Chemical Society. **(B)** Flower-like spheres. Reprinted with permission from Tu et al. (2019). Copyright (2019) American Chemical Society. **(C)** Nanorods. Reprinted with permission from Sun et al. (2018). Copyright (2018) American Chemical Society. **(D)** Porous film. Reprinted with permission from Li et al. (2019). Copyright (2019) American Chemical Society. **(E)** Porous hollow rhomboids. Reprinted with permission from Han et al. (2020). Copyright (2020) American Chemical Society.

Given this, various 2-D nanomaterials such as carbon nanotube (CNT), graphene, and molybdenum disulfide (MoS<sub>2</sub>) have been synthesized by different methods (Zhou et al., 2018e; Choi et al., 2020). As an n-type semiconductor material with wide band gap, MoS<sub>2</sub> receives the most interest because of its high surface activity and chemical stability (Fan et al., 2017; Zhang et al., 2019). Up to now, a large number of studies have been carried out on the various nanostructures of MoS<sub>2</sub>, including nanoflakes (Johari et al., 2020), nanotubes (Zhong et al., 2020), nanospheres (Li Y. X. et al., 2019) and other complex hierarchical nanostructures (Zhang et al., 2018b; Agrawal et al., 2020), to realize more effective methods of detecting SF<sub>6</sub> decomposed products. Besides, the evident correlation has been confirmed between unique structures and performances (Barzegar et al., 2019; Wang et al., 2020). Therefore, the morphology synthesis and analysis of MoS<sub>2</sub> nanostructures are of great significant to discuss. This mini review summarizes the morphological features and sensing applications of MoS<sub>2</sub>, especially for detecting SF<sub>6</sub> decomposed products.

## Morphology and analysis of MoS<sub>2</sub>

MoS<sub>2</sub> is deemed as a viable and effective material owing to its stable semiconducting property and high thermal stability (Sahoo et al., 2016; Sangeetha and Madhan, 2020). Until now, the diverse morphology of MoS<sub>2</sub> nanostructures have been designed by investigators through various methods to achieve excellent sensing properties in the aspects of chemical, optical, and gas

sensors (Zhang et al., 2018a; Bhakhar et al., 2019). Kang et al. demonstrated vertical MoS<sub>2</sub> nanoflakes (shown in **Figure 1A**) fabricated on SiO<sub>2</sub>/Si substrates by the deposition and thermal evaporation. They found the vertical flakes supplied an effective surface area and sufficient oxygen vacancies for the adsorption of NO<sub>2</sub> gas. The minimum concentration of the NO<sub>2</sub> detection was 0.15 ppm at room temperature (Kang et al., 2017). Tu et al. synthesized hierarchical MoS<sub>2</sub> spheres with flower-like structures (shown in **Figure 1B**) presented efficient aluminum storage properties. These flower-like microstructures for aluminum storage possessed open and well-defined hierarchical structures, leading to a higher specific capacity and prominent cycling stability. The as-prepared MoS<sub>2</sub> electrodes delivered reversible capacities of 112.2 mAh g<sup>-1</sup> at 153.6 mAh g<sup>-1</sup> after 100 cycles (Tu et al., 2019).

Sun et al. developed MoS<sub>2</sub> nanorods (shown in **Figure 1C**) by the hydrothermal and ammonia annealing approach and found that the fabricated nanorods exhibited excellent catalytic performances due to a more specific surface area and a sufficient ion transportation channel (Sun et al., 2018). Li et al. fabricated a three-dimensional porous MoS<sub>2</sub> film of surface-grown Pt nanocrystals (shown in **Figure 1D**) via the CVD-TA method, and found that higher Pt loading yields improved the performances of the hydrogen evolution reaction with a smaller specific surface area. Besides, these special porous constructions could effectively solve the stacking and agglomeration problems owing to the electrochemical reaction,

guarding remarkable cycling stability (Li et al., 2019). Han et al. reported electrode material performance of hierarchically porous MoS<sub>2</sub>-Carbon hollow rhomboids (shown in **Figure 1E**) prepared by a self-templated solvothermal reaction. The as-prepared electrodes delivered reversible capacities of 506 mAh g<sup>-1</sup> at 0.1 A g<sup>-1</sup> after 3,000 cycles. The authors ascribed the excellent storage energy properties of MoS<sub>2</sub>-C rhomboids structures to the distinct internal void structure (Han et al., 2020).

## MoS<sub>2</sub> SENSOR FOR SF<sub>6</sub> DECOMPOSING PRODUCTS

### Theoretical calculations about MoS<sub>2</sub>-based sensors

In order to analyze and investigate the adsorption process between SF<sub>6</sub> decomposed gases and MoS<sub>2</sub>-based material, corresponding adsorbing factors containing total adsorption energies ( $E_{ads}$ ), the value of charge transfer ( $Q_t$ ), and projected or total density of state can be attained (Azofra et al., 2017). The calculation formula is as follows:

$$E_{ads} = E_{\text{MoS}_2/\text{gas molecule}} - E_{\text{MoS}_2} - E_{\text{gas molecule}} \quad (1)$$

$E_{\text{MoS}_2/\text{gas molecule}}$  is the systemic energy after reaction,  $E_{\text{gas molecule}}$  and  $E_{\text{MoS}_2}$ , signify the energy of gas molecule and the full energies of the MoS<sub>2</sub> before the reaction, respectively (Wang et al., 2019c). The negative value of  $E_{ad}$  illustrates the exothermic procedure of gas adsorption and the spontaneity of reaction. Moreover, the charge transfer  $Q_t$  before and after the gas molecule adsorbed on the MoS<sub>2</sub> system is defined by **Eq. 2**:

$$Q_t = Q_a - Q_b \quad (2)$$

where  $Q_a$  and  $Q_b$  present the number of charge after adsorption carried by the gas and the net carried charge of isolated gas molecules, respectively (Zhao et al., 2016; Wang et al., 2019b). The negative value of  $Q_t$  presents the electrons transfer from the MoS<sub>2</sub>-based system to gas molecules.

The adsorption procedures between gas sensing materials and SF<sub>6</sub> decomposing products were studied based on the density functional theory (DFT) (Singh et al., 2018; Cui et al., 2019). For instance, Abbasi et al. studied the adsorptions properties of SO<sub>2</sub> molecules on MoS<sub>2</sub> monolayers in the aspects of charge transfer, band structures, adsorption energy, and charge density differences. They found that SO<sub>2</sub> gas molecules were adsorbed on the surface monolayer by physisorption. The S-O bonds of the adsorption gas molecules were lengthened after the adsorbed process. Furthermore, elongation of the bond lengths was mainly owed to the transfer of charge density from the original to the new bonds between the MoS<sub>2</sub> monolayers and target gas molecules, and the adsorption of SO<sub>2</sub> changed the electronic properties of MoS<sub>2</sub> monolayer (Abbasi and Sardroodi 2019). Chen et al. theoretically discussed the adsorption behavior of five types of SF<sub>6</sub> decomposing products (H<sub>2</sub>S, HF, SO<sub>2</sub>, SOF<sub>2</sub>, and SO<sub>2</sub>F<sub>2</sub>) on the MoS<sub>2</sub> monolayer by employing the NEGF combined with DFT method. Among the five types of gas molecules, MoS<sub>2</sub> monolayer had the best adsorption performance for SO<sub>2</sub> caused by the special electronegativity (Chen et al., 2019a).

**TABLE 1** | Comparison of adsorption parameters for H<sub>2</sub>S and SO<sub>2</sub> in different systems.

SF <sub>6</sub> Decomposing products	System	$E_{ad}$ (eV)	$Q_t$ (e)	References
H <sub>2</sub> S	MoS <sub>2</sub>	-0.22	0.02	Chen et al., 2019a
	Si-MoS <sub>2</sub>	-0.68	0.16	Gui et al., 2019
	Ni-MoS <sub>2</sub>	-1.319	0.254	Wei et al., 2018
	Pt-MoS <sub>2</sub>	-1.465	0.302	Qian et al., 2019
SO <sub>2</sub>	MoS <sub>2</sub>	-0.30	-0.04	Chen et al., 2019a
	Ni-MoS <sub>2</sub>	-1.382	-0.016	Wei et al., 2018
	Pt-MoS <sub>2</sub>	-1.584	0.036	Qian et al., 2019
	Al-MoS <sub>2</sub>	-2.33	-3.43	Zhang et al., 2018

In another instance, Qian et al. researched the adsorption property of H<sub>2</sub>S and SO<sub>2</sub> on the Pt-decorated MoS<sub>2</sub> and found that Pt-MoS<sub>2</sub> showed a strong interaction with gas molecules due to the strong chemical activity of with Pt atom. The adsorption energy of H<sub>2</sub>S and SO<sub>2</sub> molecules adsorbed on Pt-MoS<sub>2</sub> was -1.465 and -1.584 eV, respectively, suggesting the occurrence of strong chemisorption in the contact surfaces. The charge transfer amount between H<sub>2</sub>S and Pt-MoS<sub>2</sub> was up to 0.302 e, which is much higher than that of SO<sub>2</sub> (0.036 e). The results indicated that Pt-MoS<sub>2</sub> exhibited an excellent adsorption property for H<sub>2</sub>S gas (Qian et al., 2019). Wei et al. reported the response behavior of Ni-MoS<sub>2</sub> towards SF<sub>6</sub> typical decomposition products: SO<sub>2</sub> and H<sub>2</sub>S. The different adsorption sites for the SO<sub>2</sub> and H<sub>2</sub>S on Ni-MoS<sub>2</sub> surface were designed to find the site of optimal adsorption energy. The result of SO<sub>2</sub> and H<sub>2</sub>S was -1.382 and -1.319 eV, respectively, indicating the strong chemical interaction between the Ni-doped MoS<sub>2</sub> monolayer and two kinds of gases (Wei et al., 2018). Gui et al. reported that Si-doped MoS<sub>2</sub> were used to investigate its adsorptive properties to H<sub>2</sub>S and SOF<sub>2</sub>, and found that the most stable doping site were above the S atom. The adsorption energy was -0.68 eV when H<sub>2</sub>S adsorbed on Si-MoS<sub>2</sub>, while pristine MoS<sub>2</sub> was only -0.17 eV. The adsorption energy of SOF<sub>2</sub> adsorbed on Si-MoS<sub>2</sub> reached -3.63 eV, which was much higher than the -0.01 eV of the pristine MoS<sub>2</sub> adsorption system. The results provided that the adsorption capacities of pristine MoS<sub>2</sub> for H<sub>2</sub>S and SOF<sub>2</sub> gases could be greatly improved by doping them with a nonmetallic atom (Gui et al. 2019). Li et al. selected the Pd atom as the dopant to modify the surface of the MoS<sub>2</sub> monolayer in the latest study, and an adsorbent with higher properties for the adsorption of SOF<sub>2</sub> and SO<sub>2</sub>F<sub>2</sub> gases was obtained on this basis. In addition, the double gas molecules could still be stably adsorbed on the surface of Pd-MoS<sub>2</sub>, indicating the feasibility of the adsorbent (Li et al. 2020).

In the above, the adsorption of H<sub>2</sub>S and SO<sub>2</sub> molecules in different systems have been discussed in detail. The simulation results of H<sub>2</sub>S and SO<sub>2</sub> molecules adsorption are in **Table 1**. These values may be obtained by different DFT functions. Compared with the adsorption construction of a pristine MoS<sub>2</sub> system, the introduction of novel elements promotes the surface chemical activity of the MoS<sub>2</sub> system. In addition, the addition of dopants enhances the affect of orbital hybridization between the MoS<sub>2</sub> monolayer and gas molecules, and facilitates the electronic transfer. The

adsorption capacity of the modified materials to the goal gas will be further improved, when the dopant is suitable (Zhang et al., 2017a).

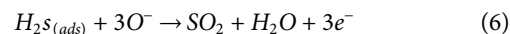
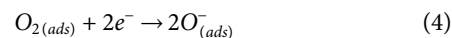
## Experimental analysis about MoS<sub>2</sub>-based sensors

At present, there are few experimental studies on the detection of SF<sub>6</sub> decomposed byproducts, the few that do mainly focus on the H<sub>2</sub>S, SO<sub>2</sub>, and CO gases (Wang et al., 2019a; Zhou et al., 2019). Park et al. prepared a MoS<sub>2</sub> gas sensor modified with Pt nanoparticles with a low detection limit and high sensitivity for H<sub>2</sub>S gas. The Pt-MoS<sub>2</sub>-based sensor reduced the minimum detection concentration of H<sub>2</sub>S gas to 5 ppm, which was much lower than that of the pure MoS<sub>2</sub> sensor (30 ppm) (Park et al., 2018). The Pt-MoS<sub>2</sub> film structures were formed by the introduction of Pt nanoparticles with ultra-small diameters, which could distinctly improve the performance of sensors. The Ni-doped MoS<sub>2</sub> nanoflower synthesized by Zhang et al. displayed a faster and higher response to 5 ppm SO<sub>2</sub> gas (Ra/Rg = 14.75) at room temperature. The main reason was that the richer porosity in the nanoflower structures provided sufficient adsorption sites for SO<sub>2</sub> gas (Zhang et al., 2017b). Hierarchical MoS<sub>2</sub> nanospheres assembled from nanosheets fabricated by Zhou et al. exhibited high properties to CO. The response value of the gas sensor to 500 ppm CO reached 92.6 at 230°C. Besides, this sensor had almost no response to other gases when the operation temperature was higher than 200°C, indicating the outstanding selectivity toward CO gas (Zhou et al., 2018c). The experimental results show that these unique nanostructures can enhance the gas-sensing performance, which is attributed to the increase of oxygen vacancies and the promotion of gas adsorption-desorption efficiency. Although some advancements have been made in the detection of SF<sub>6</sub> decomposed products, more high-accuracy experiments are needed for other decomposition gases such as SOF<sub>2</sub> and SO<sub>2</sub>F<sub>2</sub>.

## Gas sensing mechanism

The gas sensing mechanism of the MoS<sub>2</sub>-based sensors to SF<sub>6</sub> decomposed products can be explained by the change of conductivity caused by the interaction between oxyanions (mainly O<sup>-</sup>) on the material surface and target gas molecules. Firstly, the oxygen molecules in air will adsorb on the surface of semiconductor materials and capture electrons from the adsorption sites to form oxyanions. The formation of an electron depletion layer and the increase of resistance are caused by oxygen adsorption. Then, when sensors are placed in an environment of reductive gas, the test gas molecules react with oxyanions to release the electrons

back to the surface of the material, resulting in the decrease of the electron depletion layer and the occurrence of conductivity change. The relevant reactions are depicted as follows (take H<sub>2</sub>S gas as an example):



## CONCLUSION

In this paper, we focused on the morphological characteristics and application of MoS<sub>2</sub> materials for the detection of SF<sub>6</sub> decomposed products in GIS. Firstly, partial reports of sensing properties of MoS<sub>2</sub> with various morphologies were concluded. Diverse MoS<sub>2</sub> structures presented relatively different sensing properties at specific operating temperatures, so it was possible to promote sensing performances of MoS<sub>2</sub> by simple surface morphology modification. With the increasing demand for sensor materials, simple and more convenient synthetic routes and more favorable morphology structures should be proposed. Next, it was shown that the selectivity and sensitivity of MoS<sub>2</sub> gas sensors could also be enhanced by the enlargement of the active surface area and the introduction of metal or non-metal elements based on formerly theoretical and experimental investigations. Then, the gas-sensing mechanism of the MoS<sub>2</sub> based sensors to SF<sub>6</sub> decomposed products was described by comparing the characteristics of material substrate and gas molecules. Although some developments have been obtained in theoretical research into SF<sub>6</sub> decomposed products, a large number of fundamental experiments are needed to further prepare MoS<sub>2</sub> sensors for practical industrial applications.

## DATA AVAILABILITY STATEMENT

The raw data supporting the conclusions of this article will be made available by the authors, without undue reservation, to any qualified researcher.

## AUTHOR CONTRIBUTIONS

All authors listed have made a substantial, direct, and intellectual contribution to the work, and approved it for publication.

## REFERENCES

- Abbasi, A., and Sardroodi, J. J. (2019). Adsorption of O<sub>3</sub>, SO<sub>2</sub> and SO<sub>3</sub> gas molecules on MoS<sub>2</sub> monolayers: a computational investigation. *Appl. Surf. Sci.* 469, 781–791. doi:10.1016/j.apsusc.2018.11.039.
- Agrawal, A. V., Kumar, R., Yang, G., Bao, J. M., Kumar, M., and Kumar, M. (2020). Enhanced adsorption sites in monolayer MoS<sub>2</sub> pyramid structures for highly

sensitive and fast hydrogen sensor. *Int. J. Hydrog. Energy* 45 (15), 9268–9277. doi:10.1016/j.ijhydene.2020.01.119.

Azofra, L. M., Sun, C. H., Cavallo, L., and MacFarlane, D. R. (2017). Feasibility of N<sub>2</sub> binding and reduction to ammonia on Fe-deposited MoS<sub>2</sub> 2D sheets: a DFT study. *Chem. Eur. J.* 23 (24), 8275–8279. doi:10.1002/chem.201701113.

Barzegar, M., Zad, A. I., and Tiwari, A. (2019). On the performance of vertical MoS<sub>2</sub> nanoflakes as a gas sensor performance of vertical MoS<sub>2</sub> nanoflakes as a gas sensor. *Vacuum* 167, 90–97. doi:10.1016/j.vacuum.2019.05.033.

- Bhakar, S. A., Patel, N. F., Zankat, C. K., Tannarana, M., Solanki, G. K., Patel, K. D., et al. (2019). Sonochemical exfoliation and photodetection properties of MoS<sub>2</sub> nanosheets. *Mater. Sci. Semicond. Process.* 98, 13–18. doi:10.1016/j.mssp.2019.03.017.
- Chen, D. C., Tang, J., Zhang, X. X., Li, Y., and Liu, H. J. (2019a). Detecting decompositions of sulfur hexafluoride using MoS<sub>2</sub> monolayer as gas sensor. *IEEE Sens. J.* 19, 39–46. doi:10.1109/JSEN.2018.2876637.
- Chen, D. C., Zhang, X. X., Tang, J., Cui, H., and Li, Y. (2018). Noble metal (Pt or Au)-doped monolayer MoS<sub>2</sub> as a promising adsorbent and gas-sensing material to SO<sub>2</sub>, SOF<sub>2</sub>, and SO<sub>2</sub>F<sub>2</sub>: a DFT study. *Appl. Phys. A-Mater.* 124 (2), 194. doi:10.1007/s00339-018-1629-y.
- Choi, G. J., Mishra, R. K., and Gwag, J. S. (2020). 2D layered MoS<sub>2</sub> based gas sensor for indoor pollutant formaldehyde gas sensing applications. *Mater. Lett.* 264, 127385. doi:10.1016/j.matlet.2020.127385.
- Cui, H., Zhang, X. X., Zhang, G. Z., and Tang, J. (2019). Pd-doped MoS<sub>2</sub> monolayer: a promising candidate for DGA in transformer oil based on DFT method. *Appl. Surf. Sci.* 470, 1035–1042. doi:10.1016/j.apsusc.2018.11.230.
- Fan, C., Liu, G. Z., Zhang, Y. H., and Wang, M. J. (2017). Synthesis and gas-responsive characteristics to methanol and isopropanol of bean-sprout-like MoS<sub>2</sub>. *Mater. Lett.* 209, 8–10. doi:10.1016/j.matlet.2017.07.092.
- Gui, Y. G., Liu, D. K., Li, X. D., Tang, C., and Zhou, Q. (2019). DFT-based study on H<sub>2</sub>S and SOF<sub>2</sub> adsorption on Si-MoS<sub>2</sub> monolayer. *Results Phys.* 13, 1–8. doi:10.1016/j.rinp.2019.102225.
- Han, L. F., Wu, S. D., Hu, Z., Chen, M. Z., Ding, J. W., Wang, S. W., et al. (2020). Hierarchically porous MoS<sub>2</sub>-carbon hollow rhomboids for superior performance of the anode of sodium-ion batteries. *ACS Appl. Mater. Interfaces* 12 (9), 10402–10409. doi:10.1021/acsami.9b21365.
- Johari, M. H., Sirat, M. S., Mohamed, M. A., Nasir, S. N. F. M., Teridi, M. A. M., and Mohamad, A. R. (2020). Effects of Mo vapor concentration on the morphology of vertically standing MoS<sub>2</sub> nanoflakes. *Nanotechnology* 31 (30), 305710. doi:10.1088/1361-6528/ab8666.
- Kang, M. A., Han, J. K., Cho, S. Y., Bu, S. D., Park, C. Y., Myung, S., et al. (2017). Strain-gradient effect in gas sensors based on three-dimensional hollow molybdenum disulfide nanoflakes. *ACS Appl. Mater. Interfaces* 9 (50), 43799–43806. doi:10.1021/acsami.7b14262.
- Li, S., Lee, J. K., Zhou, S., Pasta, M., and Warner, J. H. (2019). Synthesis of surface grown Pt nanoparticles on edge-enriched MoS<sub>2</sub> porous thin films for enhancing electrochemical performance. *Chem. Mat.* 31 (2), 387–397. doi:10.1021/acs.chemmater.8b03540.
- Li, T., Gui, Y. G., Zhao, W. H., Tang, C., and Dong, X. C. (2020). Palladium modified MoS<sub>2</sub> monolayer for adsorption and scavenging of SF<sub>6</sub> decomposition products: a DFT study. *Physica E* 123, 114178. doi:10.1016/j.physe.2020.114178.
- Li, Y. X., Song, Z. X., Li, Y. N., Chen, S., Li, S., Li, Y. H., et al. (2019). Hierarchical hollow MoS<sub>2</sub> microspheres as materials for conductometric NO<sub>2</sub> gas sensors. *Sens. Actuators, B-Chem.* 282, 259–267. doi:10.1016/j.snb.2018.11.069.
- Liu, H. C., Zhou, Q., Zhang, Q. Y., Hong, C. X., Xu, L. N., Jin, L. F., et al. (2017). Synthesis, characterization and enhanced sensing properties of a NiO/ZnO p-n junctions sensor for the SF<sub>6</sub> decomposition byproducts SO<sub>2</sub>, SO<sub>2</sub>F<sub>2</sub>, and SOF<sub>2</sub>. *Sensors* 17 (4), 913. doi:10.3390/s17040913.
- Lu, Z. R., Zhou, Q., Wang, C. S., Wei, Z. J., Xu, L. N., and Gui, Y. G. (2018). Electrospun ZnO-SnO<sub>2</sub> composite nanofibers and enhanced sensing properties to SF<sub>6</sub> decomposition byproduct H<sub>2</sub>S. *Front. Chem.* 6, 540. doi:10.3389/fchem.2018.00540.
- Lu, Z. R., Zhou, Q., Wei, Z. J., Xu, L. N., Peng, S. D., and Zeng, W. (2019). Synthesis of hollow nanofibers and application on detecting SF<sub>6</sub> decomposing products. *Front. Mater.* 6, 183. doi:10.3389/fmats.2019.00183.
- Park, J., Mun, J. H., Shin, J. S., and Kang, S. W. (2018). Highly sensitive two-dimensional MoS<sub>2</sub> gas sensor decorated with Pt nanoparticles. *R. Soc. Open Sci.* 5 (12), 181462. doi:10.1098/rsos.181462.
- Qian, H., Lu, W. H., Wei, X. X., Chen, W., and Deng, J. (2019). H<sub>2</sub>S and SO<sub>2</sub> adsorption on Pt-MoS<sub>2</sub> adsorbent for partial discharge elimination: a DFT study. *Results Phys.* 12, 107–112. doi:10.1016/j.rinp.2018.11.035.
- Sahoo, M. P. K., Wang, J., Zhang, Y. J., Shimada, T., and Kitamura, T. (2016). Modulation of gas adsorption and magnetic properties of monolayer-MoS<sub>2</sub> by antisite defect and strain. *J. Phys. Chem. C* 120 (26), 14113–14121. doi:10.1021/acs.jpcc.6b03284.
- Sangeetha, M., and Madhan, D. (2020). Ultra sensitive molybdenum disulfide (MoS<sub>2</sub>)/graphene based hybrid sensor for the detection of NO<sub>2</sub> and formaldehyde gases by fiber optic clad modified method. *Opt. Laser Technol.* 127, 106193. doi:10.1016/j.optlastec.2020.106193.
- Singh, A. K., Kumar, P., Late, D. J., Kumar, A., Patel, S., and Singh, J. (2018). 2D layered transition metal dichalcogenides (MoS<sub>2</sub>): synthesis, applications and theoretical aspects. *Appl. Mater. Today* 13, 242–270. doi:10.1016/j.apmt.2018.09.003.
- Sun, T., Wang, J., Chi, X., Lin, Y. X., Chen, Z. X., Ling, X., et al. (2018). Engineering the electronic structure of MoS<sub>2</sub> nanorods by N and Mn dopants for ultra-efficient hydrogen production. *ACS Catal.* 8 (8), 7585–7592. doi:10.1021/acscatal.8b00783.
- Tu, J. G., Xiao, X., Wang, M. Y., and Jiao, S. Q. (2019). Hierarchical flower-like MoS<sub>2</sub> microspheres and their efficient Al storage properties. *J. Phys. Chem. C* 123 (44), 26794–26802. doi:10.1021/acs.jpcc.9b07509.
- Wang, J. X., Zhou, Q., Lu, Z. R., Gui, Y. G., and Zeng, W. (2019b). Adsorption of H<sub>2</sub>O molecule on TM (Au, Ag) doped-MoS<sub>2</sub> monolayer: a first-principles study. *Physica E* 113, 72–78. doi:10.1016/j.physe.2019.05.006.
- Wang, J. X., Zhou, Q., Lu, Z. R., Wei, Z. J., and Zeng, W. (2019c). Gas sensing performances and mechanism at atomic level of Au-MoS<sub>2</sub> microspheres. *Appl. Surf. Sci.* 490, 124–136. doi:10.1016/j.apsusc.2019.06.075.
- Wang, J. X., Zhou, Q., Xu, L. N., Gao, X., and Zeng, W. (2020). Gas sensing mechanism of dissolved gases in transformer oil on Ag-MoS<sub>2</sub> monolayer: a DFT study. *Physica E* 118, 113947. doi:10.1016/j.physe.2019.113947.
- Wang, J. X., Zhou, Q., and Zeng, W. (2019a). Competitive adsorption of SF<sub>6</sub> decompositions on Ni-doped ZnO (100) surface: computational and experimental study. *Appl. Surf. Sci.* 479, 185–197. doi:10.1016/j.apsusc.2019.01.255.
- Wei, H. L., Gui, Y. G., Kang, J., Wang, W. B., and Tang, C. (2018). A DFT study on the adsorption of H<sub>2</sub>S and SO<sub>2</sub> on Ni doped MoS<sub>2</sub> monolayer. *Nanomaterials* 8 (9), 646. doi:10.3390/nano8090646.
- Wei, Z. J., Zhou, Q., and Zeng, W. (2020). Hierarchical WO<sub>3</sub>-NiO microflower for high sensitivity detection of SF<sub>6</sub> decomposition byproduct H<sub>2</sub>S. *Nanotechnology* 31 (21), 215701. doi:10.1088/1361-6528/ab73bd.
- Zeng, F., Ju, T., Zhang, X., Pan, J., Qiang, Y., and Hou, X. (2015). Influence regularity of trace H<sub>2</sub>O on SF<sub>6</sub> decomposition characteristics under partial discharge of needle-plate electrode. *IEEE T. Dielect. El. In.* 22 (1), 287–295. doi:10.1109/TDEI.2014.004217.
- Zhang, D. Z., Jiang, C. X., Li, P., and Sun, Y. (2017a). Layer-by-layer self-assembly of Co<sub>3</sub>O<sub>4</sub> nanorod-decorated MoS<sub>2</sub> nanosheet-based nanocomposite toward high-performance ammonia detection. *ACS Appl. Mater. Inter. Interfaces* 9 (7), 6462–6471. doi:10.1021/acsami.6b15669.
- Zhang, D. Z., Wu, J. F., Li, P., and Cao, Y. H. (2017b). Room temperature SO<sub>2</sub> gas-sensing properties based on a metal-doped MoS<sub>2</sub> nanoflower: an experimental and density functional theory investigation. *J. Mater. Chem. Am.* 5 (39), 20666–20677. doi:10.1039/c7ta07001b.
- Zhang, R. Y., Fu, D., Ni, J. M., Sun, C. B., and Song, S. X. (2018). Adsorption for SO<sub>2</sub> gas molecules on B, N, P and Al doped MoS<sub>2</sub>: the DFT study. *Chem. Phys. Lett.* 715, 273–277. doi:10.1016/j.cplett.2018.11.054.
- Zhang, S., Zhang, W., Nguyen, T. H., Jian, J., and Yang, W. (2019). Synthesis of molybdenum diselenide nanosheets and its ethanol-sensing mechanism. *Mater. Chem. Phys.* 222, 139–146. doi:10.1016/j.matchemphys.2018.08.062.
- Zhang, X. X., Chen, D., Cui, H., Dong, X., Xiao, S., and Tang, J. (2017a). Understanding of SF<sub>6</sub> decompositions adsorbed on cobalt-doped SWCNT: A DFT study. *Appl. Surf. Sci.* 420, 371–382. doi:10.1016/j.apsusc.2017.05.163.
- Zhang, X. X., Cui, H., and Gui, Y. G. (2017b). Synthesis of graphene-based sensors and application on detecting SF<sub>6</sub> decomposing products: a review. *Sensors* 17 (2), 363. doi:10.3390/s17020363.
- Zhang, Y. J., Zeng, W., and Li, Y. Q. (2018a). Hydrothermal synthesis and controlled growth of hierarchical 3D flower-like MoS<sub>2</sub> nanospheres assisted with CTAB and their NO<sub>2</sub> gas sensing properties. *Appl. Surf. Sci.* 455, 276–282. doi:10.1016/j.apsusc.2018.05.224.
- Zhang, Y. J., Zeng, W., and Li, Y. Q. (2018b). The hydrothermal synthesis of 3D hierarchical porous MoS<sub>2</sub> microspheres assembled by nanosheets with excellent gas sensing properties. *J. Alloys Compd.* 749, 355–362. doi:10.1016/j.jallcom.2018.03.307.
- Zhao, B., Li, C. Y., Liu, L. L., Zhou, B., Zhang, Q. K., Chen, Z. Q., et al. (2016). Adsorption of gas molecules on Cu impurities embedded monolayer MoS<sub>2</sub>: a first-principles study. *Appl. Surf. Sci.* 382, 280–287. doi:10.1016/j.apsusc.2016.04.158.
- Zhong, Y. L., Liu, D., Wang, L. T., Zhu, H. G., and Hong, G. (2020). Controllable synthesis of hierarchical MoS<sub>2</sub> nanotubes with ultra-uniform and superior storage potassium properties. *J. Colloid Interface Sci.* 561, 593–600. doi:10.1016/j.jcis.2019.11.034.

- Zhou, Q., Chen, W. G., Li, J., Peng, S. D., Lu, Z. R., Yang, Z., et al. (2018b). Highly sensitive hydrogen sulfide sensor based on titanium dioxide nanomaterials. *J. Nanoelectron. Optoelectron.* 13 (12), 1784–1788. doi:10.1166/jno.2018.2417.
- Zhou, Q., Chen, W. G., Xu, L. N., Kumarc, R., Gui, Y. G., Zhao, Z. Y., et al. (2018a). Highly sensitive carbon monoxide (CO) gas sensors based on Ni and Zn doped SnO<sub>2</sub> nanomaterials. *Ceram. Int.* 44 (4), 4392–4399. doi:10.1016/j.ceramint.2017.12.038.
- Zhou, Q., Hong, C. X., Yao, Y., Hussain, S., Xu, L. N., Zhang, Q. Y., et al. (2018c). Hierarchically MoS<sub>2</sub> nanospheres assembled from nanosheets for superior CO gas-sensing properties. *Mater. Res. Bull.* 101, 132–139. doi:10.1016/j.materresbull.2018.01.030.
- Zhou, Q., Umar, A., Sodki, E. M., Amine, A., Xu, L. N., Gui, Y. G., et al. (2018d). Fabrication and characterization of highly sensitive and selective sensors based on porous NiO nanodisks. *Sens. Actuator B-Chem.* 259, 604–615. doi:10.1016/j.snb.2017.12.050.
- Zhou, Q., Xu, L. N., Umar, A., Chen, W. G., and Kumar, R. (2018e). Pt nanoparticles decorated SnO<sub>2</sub> nanoneedles for efficient CO gas sensing applications. *Sens. Actuator B-Chem.* 256, 656–664. doi:10.1016/j.snb.2017.09.206.
- Zhou, Q., Zeng, W., Chen, W. G., Xu, L. N., Kumarc, R., and Umar, A. (2019). High sensitive and low-concentration sulfur dioxide (SO<sub>2</sub>) gas sensor application of heterostructure NiO-ZnO nanodisks. *Sens. Actuator B-Chem.* 298, 126870. doi:10.1016/j.snb.2019.126870.

**Conflict of Interest:** Authors GQ, QP, DZ, SW, and BY were employed by the Electric Power Science Research Institute of Yunnan Power Grid Co., Ltd.

Copyright © 2020 Qian, Peng, Wang, Wang and Dai. This is an open-access article distributed under the terms of the Creative Commons Attribution License (CC BY). The use, distribution or reproduction in other forums is permitted, provided the original author(s) and the copyright owner(s) are credited and that the original publication in this journal is cited, in accordance with accepted academic practice. No use, distribution or reproduction is permitted which does not comply with these terms.